Journal of Natural Gas Science and Engineering 52 (2018) 94–105

Contents lists available at ScienceDirect

Journal of Natural Gas Science and Engineering

journal homepage: www.elsevier.com/locate/jngse

Response of natural gas distribution pipeline networks to ambient temperature variation (unsteady simulation)

Mahmood Farzaneh-Gord, Hamid Reza Rahbari*

The Faculty of Mechanical Engineering, Shahrood University of Technology, Shahrood, Iran

ARTICLE INFO

Keywords:
Natural gas
Distribution pipeline network
Ambient temperature variation (ATV)
Demand forecasting
MLP neural network
Natural gas composition

ABSTRACT

Natural gas is transported through pipeline networks such as transmission and distribution to the final consumers. Local natural gas companies should make the continuous delivery of natural gas under any ambient temperature and demand. Natural gas demand varies due to ambient temperature variation (ATV) in different seasons or even during a day. The continuous supply of natural gas could be achieved only if the response of natural gas pipeline network to ATV is fully studied and understood. This study investigated the response of a typical natural gas distribution pipeline network to ATV. Firstly, a multilayer perceptron neural network model has been developed to forecast natural gas demand at any ambient temperature. Secondly, a new approach has been presented to simulate the natural gas distribution pipeline network in unsteady conditions. This approach is developed to predict the response of the distribution pipeline to ATV. The city of Semnan, Iran, was selected as the case study. Natural gas consumption in 4 coldest days of a year was extracted from the metering points. According to the results, the forecast data for natural gas demand has about 1% division compared with the actual values. Also, the node pressures significantly dropped on the coldest day of the year due to the increase in natural gas demand. In addition, the effect of natural gas composition on node pressure investigated. Results show that the natural gas with higher molecular weight has a lower pressure in all network nodes.

1. Introduction

After being extracted from wells and refined in refineries, natural gas reaches to the final consumers through pipeline networks. The natural gas pipeline networks include pipes, valves, compressors etc. and it is divided into two general categories. The first category is a high pressure natural gas transmission pipeline networks. These networks transfer natural gas to the main gate of cities. The second category is the natural gas distribution pipeline networks in which natural gas flows at medium or low pressure. These networks deliver natural gas to end costumers. Due to the long path and pressure drop in the transmission networks, compressor stations are installed at a distance of 100–150 km apart. These stations consist of a set of compressors which are responsible for increasing natural gas pressure. Natural gas could not be consumed at the pressure level with which it reaches the main gate of cities. Therefore, firstly this pressure is reduced at pressure reduction stations, and then, it is delivered to consumers by distribution networks. The main consumers of natural gas distribution networks could be classified into residential consumers (household hot water, cooking and space heating), commercial consumers (hotels, hospitals, restaurants, cinemas and etc.) and industrial customers (power plants, cement factories and etc.).

In natural gas distribution pipeline networks, the junction of two pipes is commonly called node. In addition, each distribution network is made up of several closed loops. Due to the different rate of consumption of various areas, consumption of natural gas should be specified for each node (usually called node demand). To ensure continuous supply of natural gas in any cases including natural gas consumption variation or sudden natural gas pipeline failure, natural gas distribution pipeline networks should be analyzed in unsteady (transient) conditions. For this purpose, firstly, the pipelines as the most important component of networks should be analyzed in unsteady conditions. Then, natural gas pipeline networks should be studied.

Numerous previous studies have provided algorithms and numerical methods for analyzing the unsteady (transient) flow in natural gas pipelines. These methods were based on computational fluid dynamics (CFD) methods (Greyvenstein, 2002; Ibraheem and Adewumi, 1996; Luongo and others, 1986; Osiadacz, 1983; Wylie and Streeter, 1993; Yow, 1971). Since CFD methods are time-consuming, researchers have developed other algorithms to analyze the unsteady flow in natural gas pipeline networks with simpler procedures. Researchers such as Luongo and others (1986) and Wylie et al. (1971) neglected one term (intertie

* Corresponding author.
E-mail addresses: mgord@shahroodut.ac.ir, mahmood.farzaneh@yahoo.co.uk (M. Farzaneh-Gord), rahbarihamidreza@yahoo.com (H.R. Rahbari).

https://doi.org/10.1016/j.jngse.2018.01.024
Received 4 June 2017; Received in revised form 6 January 2018; Accepted 12 January 2018
1875-5100/ © 2018 Elsevier B.V. All rights reserved.

term) in the momentum equation to achieve a simpler nonlinear governing equation of natural gas flow by linearization of these equations. Yow (1971) applied the method of characteristics to formulate the unsteady natural gas flow by considering the inertia term in the momentum equation.

Some researchers simulated unsteady natural gas pipeline network in isothermal conditions. For instance, Osiadacz (1987) and Kiuchi (1994) analyzed unsteady natural gas pipeline network by considering all terms in the momentum equation. In other studies, researchers investigated the effect of the non-isothermal condition on unsteady natural gas pipeline networks. They formulated the governing equations by applying the total variation diminishing (TVD) method (Adewumi and Zhou, 1995; Dukhovnaya and Adewumi, 2000). Moreover, Osiadacz and Chaczykowski (Osiadacz and Chaczykowski, 2001) compared the effects of isothermal and non-isothermal conditions on unsteady natural gas pipeline networks.

Tentis et al. (2003) simulated slow and fast transient conditions for natural gas flow in pipelines. Furthermore, Gato and Henriques (Gato and Henriques, 2005) applied the Galerkin method together with Runge–Kuttato simulate unsteady, one-dimensional and compressible flow in natural gas pipelines. The effect of the equation of state on momentum and energy equations in addition to the effect of thermal model on energy equation were investigated by Chaczykowski (Chaczykowski, 2010, 2009). An equation to calculate the unsteady natural gas volumetric flow rate of a pipeline based on the well-known Weymouth equation was also presented by researchers (Adeosun et al., 2009; Olatunde et al., 2012). Ebrahimzadeh et al. (2012) applied a new approach (orthogonal collocation method) to simulate the unsteady transmission pipeline network in isothermal and non-isothermal conditions. Helgaker et al. (2014)applied the GERG 2004 equation of state and simulated natural gas pipelines in unsteady conditions. In addition, Wang et al. (2015) presented four forms of governing equations of unsteady natural gas pipelines and compared the equations in terms of accuracy and efficiency.

A Few studies have been conducted in the field of unsteady natural gas pipeline networks. Electrical circuits are employed to simulate unsteady natural gas pipeline networks in isothermal conditions (Ke and Ti, 2000; Tao and Ti, 1998). Reddy et al. (2006) developed a mathematical method to simulate unsteady natural gas pipeline network and compared it with numerical methods such as finite difference. Some investigators applied MATLAB® Simulink library to simulate natural gas distribution pipeline networks (Herrán-González et al., 2009) and natural gas pipelines (Behbahani-Nejad and Bagheri, 2010). The results show that the suggested method is more accurate and efficient than the previous studies.

In recent years, limited studies have been conducted to expand and present new approaches to simulate unsteady natural gas pipeline networks. For example, Behbahani-Nejad and Shekari (2010) developed a novel method according to corresponding Eigen system to study the governing equations. Alamian et al. (2012) employed control approaches such as state space model. In their study, the proposed model was compared with other methods, e.g. conventional, implicit, and explicit finite difference. Furthermore, Behrooz and Bozorgmehry (2015) solved the governing equations of unsteady and non-isothermal flow inside the transmission natural gas pipeline networks by presenting a new efficient procedure and method.

Literature reviews have indicated that there are three models for forecasting energy and natural gas demand: time series (TS) model, regression model (RM) and artificial neural network (ANN) (Aydinalp-Koksal and Ugursal, 2008; Kavaklioglu et al., 2009). In the TS model, energy demand is forecasted by the future data based on previously observed values. The RM is very useful for forecasting energy demand and could be linear or nonlinear based values. The ANN is new computational method for solving nonlinear problems, optimization, forecasting, etc. The main idea of the ANN is based on the human nervous system. Numerous researchers developed ANN model to forecast natural gas demand. For example, Khotanzad et al. (2000) combined two-stage ANN to forecast natural gas consumption. Potočnik et al. (2014) studied the effect of various ANN methods in forecasting residential natural gas demand in Croatia and concluded that the adaptive linear model is better than the other models. Yu and Xu (2014) developed an optimized genetic algorithm and ANN with back propagation (BP) algorithm to forecast natural gas demand. Also, some researchers from Turkey applied ANNs to forecast natural gas consumption in Ankara Province (Gorucu, 2004) and Istanbul (DEMİREL et al., 2012; Kizilaslan and Karlik, 2009). In one study, a genetic algorithm was developed to forecast natural gas consumption using ANN and for a steel plant (Kovačič and Šarler, 2014). Moreover, multilayer perceptron model (MLP) in different modes was applied by Szoplik (2015) to forecast natural gas consumption in Szczecin. In that particular study, an efficient MLP was proposed using the trial and error method.

Due to the high demand for space heating in low ambient temperatures, natural gas consumption in cities is highly influenced by ambient temperature variation. To ensure a continuous supply of natural gas, it is necessary that local natural gas companies should be able to accurately predict the natural gas consumption rate of their customers. The companies should also know the specific response of natural gas distribution pipeline networks to ATV. This response includes the node pressure at any point of the network. In cold days, the response of distribution pipeline networks to ATV is pressure drop at the nodes due to increase in natural gas demand. If the ambient temperature drop is severe, the pressure drop in the nodes and pipelines is considerable which may be resulted to the natural gas supply operation cut off. Therefore, the response of distribution network to ATV is of special importance.

Thus in this study, firstly a neural network has been developed and presented to forecast natural gas demand in a distribution pipeline network due to ATV. Then, a novel approach has been proposed to analyze the unsteady simulation of the distribution pipeline network. Finally, the response of the distribution pipeline network to ATV has been investigated. Semnan, the capital city of Semnan Province, Iran, has been selected as the case study and the effect of ATV and natural gas compositions on the studied distribution pipeline network are investigated.

2. Problem description

The city gate station (CGS) is a pressure reduction point in transmission pipeline networks with high pressure natural gas (5000–7000 kPa) at its entrance. The natural gas pressure at the CGS exit should be around 1724 kPa (250 psi). This medium pressure natural gas is transferred to the town border station (TBS) using a basic grid pipeline as part of the distribution network. The pipeline, nodes and closed loop are the main components of the distribution pipeline network. Fig. 1 and Table 1 demonstrate the details of natural gas distribution pipeline network for the case under investigation (i.e. Semnan). The natural gas demand at each node is depicted in Table 2. These informations are provided by Semnan Gas Company.

3. Natural gas demand in Semnan as case study

Natural gas consumption is influenced by climatic characteristics, e.g. daily effective temperature, cloudiness, rainfall and wind speed. These parameters, together with average ambient temperature, are usually measured, calculated and reported by local weather organizations. Fig. 2 presents the variation of average ambient temperature versus month for 2011–2013 in Semnan (I.R.OF IRAN Meteorological Organization website).

The number of natural gas consumers for Semnan, between 2011 and 2013, was approximately 45,311. Space heating, domestic hot water and cooking are the important sources of natural gas consumption. The monthly natural gas consumption was measured using

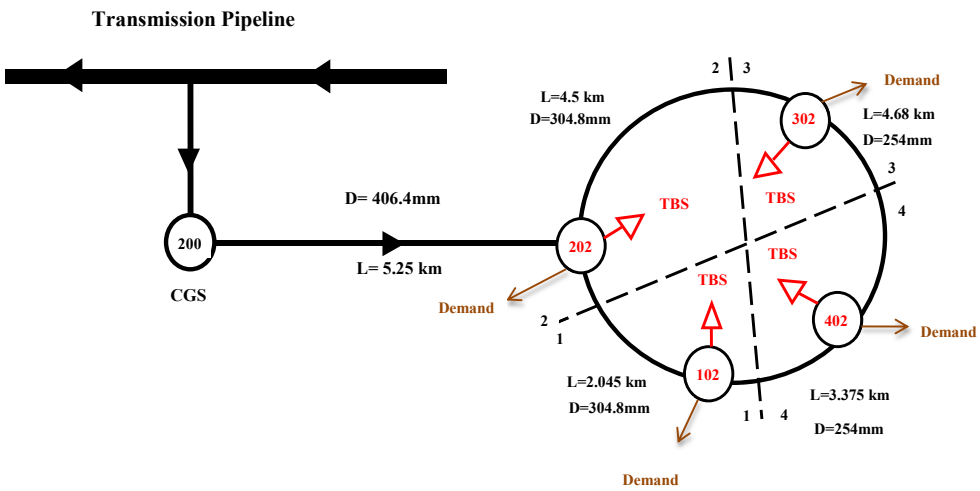

Fig. 1. The natural gas distribution pipeline network under investigation.

Table 1
Information on the natural gas distribution network under study.

Gas pipe ID	from node	to node	diameter (mm)	length (km)
0	200	202	406.4	5.250
1	202	102	304.8	2.045
2	202	302	304.8	4.5
3	302	402	254	4.68
4	102	402	254	3.375

Table 2
Natural gas demand for each node in the steady state condition.

Node	demand (m^3/h)
102	5000
202	5000
302	5000
402	16300

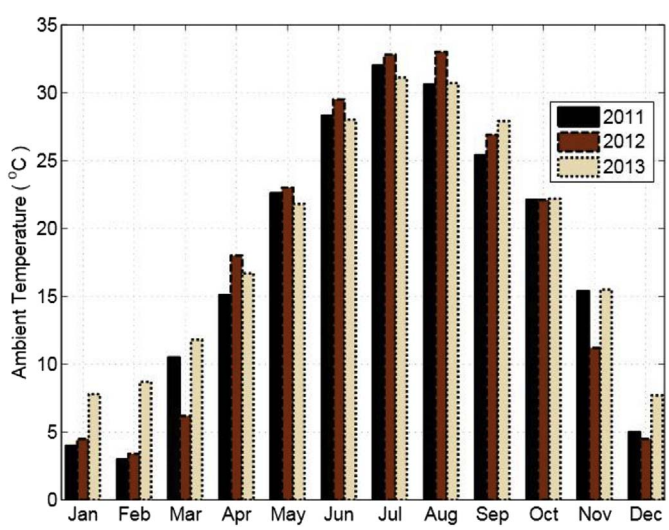

Fig. 2. Variation of ambient temperature versus month in 2011–2013 (I.R.OF IRAN Meteorological Organization website).

appropriate flow meters installed in CGS and TBS stations. Fig. 3 illustrates the natural gas consumption per user versus month for 2011–2013 (National Iran Gas Company official website).

It should be noted from Fig. 3 that, the natural gas consumption

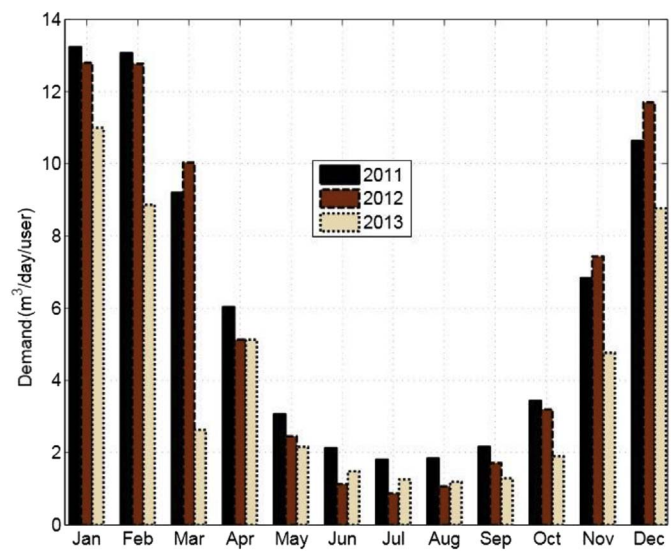

Fig. 3. Variation of natural gas consumption versus month in 2011–2013 for Semnan (National Iran Gas Company official website).

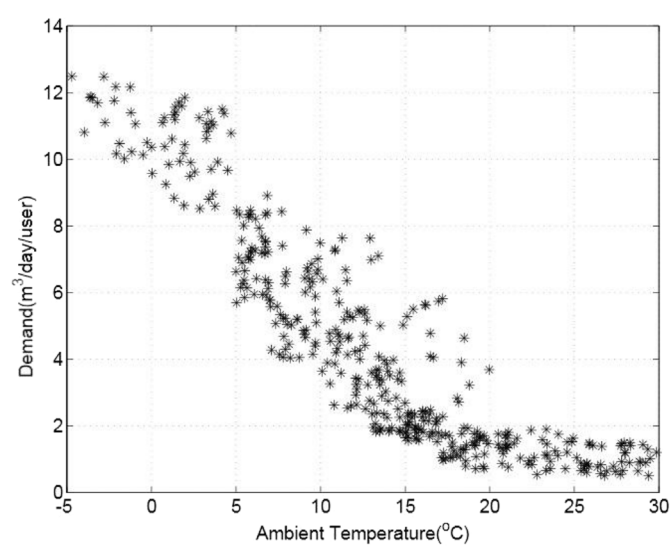

Fig. 4. Natural gas consumption versus ambient temperature during 2011–2013 (National Iran Gas Company official website).

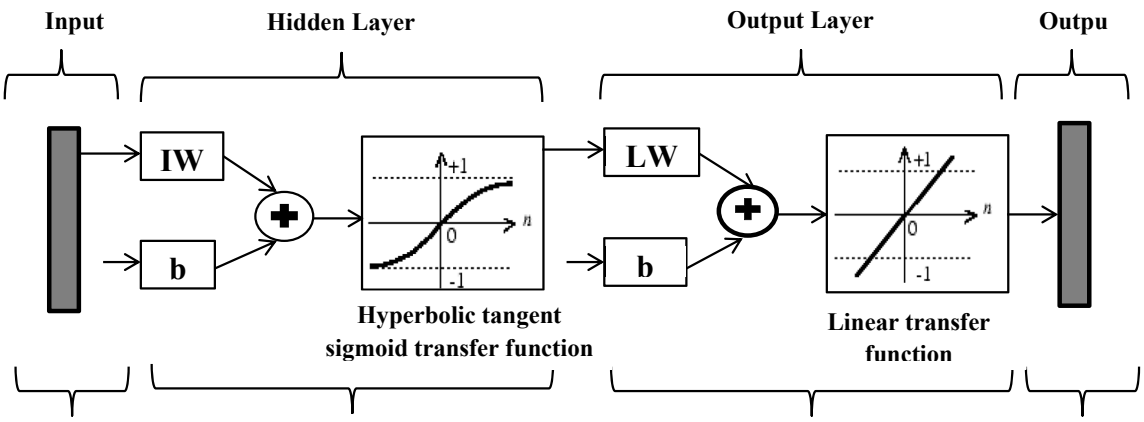

Fig. 5. MLP neural network feed-forward diagram.

increases dramatically in cold months and decreases sharply in hot months. This shows that the major consumption of natural gas in Semnan city is space heating (see Fig. 3). Fig. 4 shows the natural gas demand versus average ambient temperature during 2011–2013. According to Fig. 4, as the temperature increases, the natural gas consumption significantly reduces until 15 °C. Then, by increasing the temperature, natural gas consumption remains nearly constant. According to Fig. 4, by decreasing the average ambient temperature during the coldest days of the year, natural gas consumption increases compared with the standard mode (average).

4. Natural gas demand forecasting

As previously discussed, changes in climatic conditions resulted to variations in natural gas demand. Consequently, it is essential to develop a model for forecasting natural gas demand due to climatic conditions, especially the average ambient temperature. In the present study, a model was developed using ANN to forecast natural gas demand at any average ambient temperature.

The ANN model was used for classification and forecasting of data so that the relationships between the data are nonlinear. ANN is a simple mathematical expression of the human brain which could be used as a capable tool with various inputs and outputs. One of the easiest and most efficient arrangements proposed for use in modeling real neurons is the multilayer perceptron (MLP) model. The MLP structure contains an input layer, one or more hidden layers and one output layer. The MLP structure is also known as the feed-forward neural network because the direction of data flow is unique, from the input layer to the output layer.

The back-propagation learning algorithm is utilized to train the MLP network. It is a least mean square method which is normally employed in engineering. In a multilayer perceptron, each neuron of a layer is linked to all neurons of the previous layer. Each layer output acts as input for the following neurons. In order to train the multilayer feed-forward neural network, the back-propagation law is used. The weights are numerical values and show the intensity of each connection.

The transfer function is a mathematical equation that determines the relationship between the output neuron and the network. It demonstrates the degree of non-linearity in each neural network. The inner transfer function has been utilized by the neuron to calculate one output from a variety of inputs. This transfer function is defined as follows:

$$y = f\left(\sum_{i=1}^{N} w_i x_i\right) \tag{1}$$

In Equation (1), $w_i$is a weight for an input x_i and $N$is the number of data.

Any function could be used as a transfer function. In practice, however, a limited number of functions are utilized as the transfer function. The transfer function is considered similar in all the hidden layers. In addition, for all output-layer neurons, a type transfer function has been used. In this study, for hidden-layer neurons, the hyperbolic tangent function have been employed as the transfer function (Equation (2)) and linear functions has been used as the transfer function for output-layer neurons (Equation (3)):

$$f(x) = \frac{2}{(1 + e^{-2x})} - 1 \tag{2}$$

$$g(x) = x \tag{3}$$

In this study, the MLP neural network was applied using MATLAB® software to forecast natural gas demand. Trial and error in each layer shows that the perception with two hidden layers and15 nodes in each layer can provide an acceptable estimation. Thus, a network {29-15-15-1} with hyperbolic tangent functions in two hidden layers and linear function in the output layer has been developed to forecast hourly natural gas demand. At the input, meteorological parameters (i.e. daily effective temperature, cloudiness, rain rate and wind velocity) and gas consumption for the previous five days were fixed. The meteorological parameters for the prediction day were also considered as the network input. The 29 desired network inputs were considered. Fig. 5 illustrates the diagram of MLP neural network used in this study.

Fig. 6 presents the natural gas demand per user for actual data and forecasted data provided by the MLP neural network during a few days

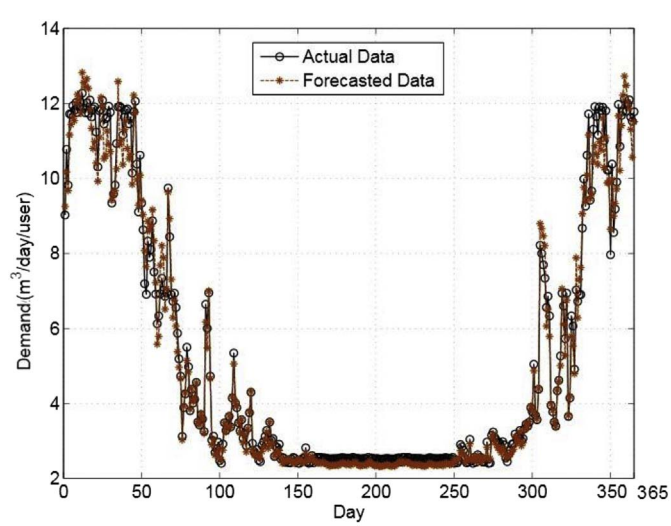

Fig. 6. The actual and forecasted natural gas demand in 2013.

in 2013. In Fig. 6, IW is the input weight matrix, LW denotes layer weight matrices and b indicates the bias vector.

The mean square error (MSE) of forecasted data has been calculated by the following equation:

$$MSE = \frac{1}{N}\sum_{i=1}^{N}\left(NGD_{act_i} - NGD_{fcst_i}\right)^2 \tag{4}$$

Regression values (R-squared) measuring the correlation between outputs and targets has been calculated as follows:

$$R - squared = \frac{N\sum_{i=1}^{N}(NGD_{act_i}NGD_{fcst_i}) - \sum_{i=1}^{N}NGD_{act_i}\sum_{i=1}^{N}NGD_{fcst_i}}{\sqrt{N\sum_{i=1}^{N}(NGD_{act_i})^2 - (\sum_{i-1}^{N}NGD_{act_i})^2} \times \sqrt{N\sum_{i=1}^{N}(NGD_{fcst_i})^2 - (\sum_{i-1}^{N}NGD_{fcst_i})^2}} \tag{5}$$

In Equations (4) and (5), N is the number of data, NGD_{act} shows the actual natural gas demand, and NGD_{fcst} denotes the forecasted natural gas demand.

In this study, the value of MSE was found to be 1.017% and the value of R-squared was calculated as 0.98. Based on these values, it could be concluded that the developed model is accurate and acceptable.

5. Mathematical modeling of the natural gas pipeline network

Here, to analyze the natural gas pipeline network, the pipeline as the most important component of the network is simulated firstly for steady and unsteady conditions. In the next step, the simulation procedure has been extended to model the distribution pipeline network as a whole for both steady and unsteady conditions. For the steady condition, a well-known model has been applied and for the unsteady condition, a new approach has been employed to simulate the distribution natural gas pipeline network. The complete mathematical modeling is discussed in this section.

5.1. Steady state pipeline network

The fundamental flow equation is the basic equation for the relationship between pressure drop and flow rate. This equation for the steady state isothermal flow in a natural gas pipeline is defined as follows (Shashi Menon, 2005):

$$Q = 1.329 \times 10^{-8}\left(\frac{T_b}{P_b}\right)\sqrt{\frac{(P_1^2 - P_2^2)}{fLZT\gamma_g}D^5} \tag{6}$$

In Equation (6), Q is the volumetric natural gas flow rate, D denotes the diameter, L shows the pipe segment length, T indicates the average flowing temperature, P_1 is the inlet pressure, P_2 denotes the outlet pressure, Z indicates the natural gas compression factor, f shows the Moody friction factor (calculated by Haaland equation), γ_g is the gas specific gravity and T_b, P_b are base temperature and pressure, respectively.

The Moody friction factor was calculated by the Haaland equation (Haaland, 1983):

$$\frac{1}{\sqrt{f}} = -\left(\frac{1.8}{n}\right)\log\left[\left(\frac{6.9}{\mathrm{Re}}\right)^n + \left(\frac{\varepsilon}{3.75D}\right)^{1.11n}\right] \tag{7}$$

Where, Re is Reynolds number, n = 3 and ε is the pipe roughness.

The fundamental flow equation (Equation (6)) could written as follows:

$$P_1^2 - P_2^2 = K\ Q^2 \tag{8}$$

In which, K is a function of pipeline properties such as length, diameter and defined as the following equation:

$$K(t) = \left(\frac{P_b}{1.329 \times 10^{-8}T_b}\right)^2\left(\frac{fLZT\gamma_g}{D^5}\right) \tag{9}$$

To analyze the natural gas pipeline network, a well-known model was developed using Kirchhoff's laws. Kirchhoff's first law says: "the algebraic sum of natural gas flow entering or leaving at each node is equal to zero."

$$\sum_{i=1}^{n} Q_i = 0 \tag{10}$$

Where, n is the number of flows entering or leaving each node and Q is the natural gas flow. The natural gas flow sign is assumed opposite for entering flows and negative for leaving flows.

Equation (11) presents the mathematical expression of Kirchhoff's second law.

$$\sum_{i=1}^{n}(P_1^2 - P_2^2)_i = 0 \tag{11}$$

In which, n is the number of nodes in each closed loop. Kirchhoff's second law should be applied for every closed loop of the network. It expresses: "For an arbitrary direction, the algebraic sum of pressure drop around the loop is equal to zero."

Fig. 7 depicts a typical natural gas pipeline network in the steady state condition. This network consists of five nodes and one closed loop. The system of Nonlinear Equation (12) have been obtained for this pipeline network in the steady condition by applying Equation (10) for each node and Equation (11) for the closed loop.

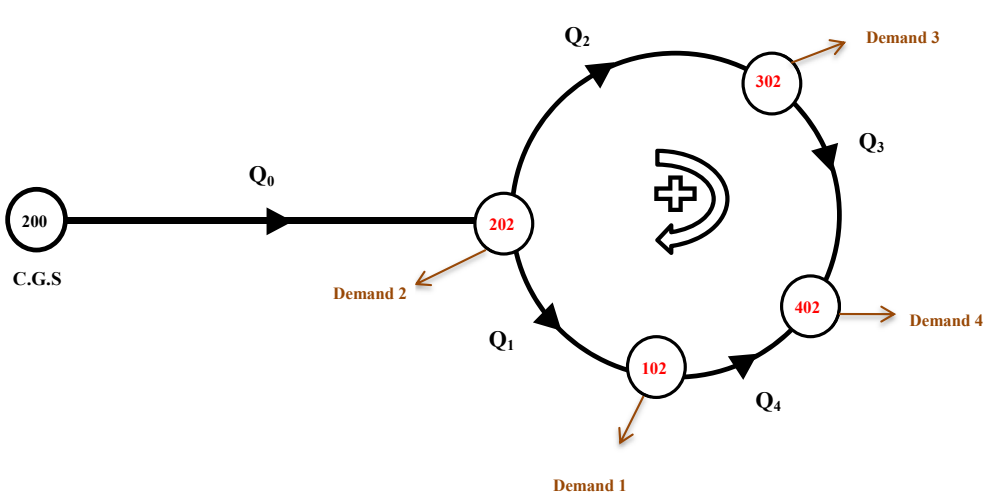

Fig. 7. The pipeline network under the steady-state condition.

$$Q_0 = Q_1 + Q_2$$
$$Q_2 = Q_3 + Demand_3$$
$$Q_1 = Q_4 + Demand_1$$
$$Q_3 + Q_4 = Demand_4$$
$$K_2\ Q_2^2 + K_3\ Q_3^2 - K_4\ Q_4^2 - K_1\ Q_1^2 = 0 \tag{12}$$

The system of Nonlinear Equation (12) have been solved by applying MATLAB® software as well as Optimization Toolbox. Natural gas flow rate (volumetric) in each pipeline was calculated by solving the system of Nonlinear Equation (12). The pressure at the nodes was calculated by determining the volumetric flow rate and applying Equation (8).

5.2. Unsteady pipeline network

The momentum equation for gas flow in the pipeline under the unsteady conditions could be presented as follows (Farzaneh-Gord and Rahbari, 2016):

$$\frac{\partial(\rho u)}{\partial t} + \frac{\partial(\rho u^2)}{\partial x} + \frac{\partial P}{\partial x} = -\frac{f\rho u^2}{2D} \tag{13}$$

Here, $\rho$is the density, u denotes the velocity, Pindicates the pressure, f refers to the Moody friction factor and $D$is the pipeline diameter. With the derivative respect to position x and time t and introducing field units, the 1D form of the energy equation for gas flow could be written as follows (Farzaneh-Gord and Rahbari, 2016):

$$\frac{dP}{dx} = -\frac{\rho}{g_c}\frac{du}{dt} - \frac{\rho u}{g_c}\frac{du}{dx} - \frac{f\rho u^2}{2g_c D} \tag{14}$$

Applying the Kolomogorov and Fomin (1957) transformation method and considering that the velocity terms have the same order, Equation (14) becomes:

$$\frac{dP}{dx} = -\frac{\rho u}{g_c}\frac{du}{dt} - \frac{\rho u}{g_c}\frac{du}{dx} - \frac{f\rho u^2}{2g_c D} \tag{15}$$

Where, g_c is the gravitational conversion factor that equals 1 in the SI unit. Equation (15) can be rewritten in the following form (Farzaneh-Gord and Rahbari, 2016):

$$\frac{1}{\rho}\frac{dP}{dx} = -\frac{u}{g_c}\frac{du}{dt} - \frac{u}{g_c}\frac{du}{dx} - \frac{fu^2}{2g_c D} \tag{16}$$

For real gases, ρ could be written in the following form:

$$\rho = \frac{Mw_a P\gamma_g}{ZRT} \tag{17}$$

In Equation (17), Mw_a represents the molecular weights of air, Z is the compression factor of natural gas, γ_g is gas specific gravity, Trefers to the temperature and Rshows the gas constant. According to the volumetric mass flow rate, velocity could be defined as follows:

$$u = (Q)\left(\frac{T}{T_b}\right)\left(\frac{P_b}{P}\right)\left(\frac{Z}{1}\right)\left(\frac{4}{\pi}\right)\left(\frac{1}{D^2}\right) \tag{18}$$

In Equation (18), Q is the volumetric gas flow rate and T_b, P_b are temperature and pressure in the base condition respectively. Here, the base condition are assumed as $T_b = 25\,^\circ\mathrm{C}$ (298.15 K) and $P_b = 101.325$ kPa (Standards and Research Department, 2003). By substituting Equations (17) and (18) into Equation (16), the following equation could be obtained:

$$\left(\frac{RZT}{Mw_a\gamma_g}\right)\frac{dP}{P} = -\frac{1}{2g_c}\left(\frac{4QTP_bZ}{\pi T_b PD^2}\right)^2\frac{dx}{dt} - \frac{1}{2g_c}\left(\frac{4QTP_bZ}{\pi T_b PD^2}\right)^2 - \frac{f}{2g_c}\left(\frac{4QTP_bZ}{\pi T_b PD^2}\right)^2\frac{dx}{D} \tag{19}$$

By arranging Equation (19), the following equation is derived:

$$\left(\frac{RZT}{Mw_a\gamma_g}\right)PdPdt = -\frac{1}{2g_c}\left(\frac{4QTP_bZ}{\pi T_b D^2}\right)^2 dx - \frac{1}{2g_c}\left(\frac{4QTP_bZ}{\pi T_b D^2}\right)^2 dt - \frac{f}{2g_c}\left(\frac{4QTP_bZ}{\pi T_b D^2}\right)^2\frac{dxdt}{D} \tag{20}$$

By integrating Equation (20) respect to time t , pressure P and position x, Equation (21) could be obtained:

$$\int_t\int_P\left(\frac{RZT}{Mw_a\gamma_g}\right)PdPdt = -\int_t\int_x\frac{1}{2g_c}\left(\frac{4QTP_bZ}{\pi T_b D^2}\right)^2 dx - \int_t\int_x\frac{1}{2g_c}\left(\frac{4QTP_bZ}{\pi T_b D^2}\right)^2 dt - \int_t\int_x\frac{f}{2g_c}\left(\frac{4QTP_bZ}{\pi T_b D^2}\right)^2\frac{dxdt}{D} \tag{21}$$

In the first step, Equation (21) integrate respect to time t as:

$$\int_P\left(\frac{RZT}{Mw_a\gamma_g}\right)PdP\int_0^t dt = -\int_x\frac{1}{2g_c}\left(\frac{4QTP_bZ}{\pi T_b D^2}\right)^2 dx - \frac{1}{2g_c}\left(\frac{4QTP_bZ}{\pi T_b D^2}\right)^2\int_0^t dt - \int_x\frac{f}{2g_c D}\left(\frac{4QTP_bZ}{\pi T_b D^2}\right)^2 dx\int_0^t dt \tag{22}$$

And in the second step, integrate respect to pressure P for left hand side and integrate respect to position x for right hand side, equation (21) becomes:

$$\left(\frac{RZT}{Mw_a\gamma_g}\right)\int_{P_1}^{P_2}PdP\int_0^t dt = -\frac{1}{2g_c}\left(\frac{4QTP_bZ}{\pi T_b D^2}\right)^2\int_0^L dx - \frac{1}{2g_c}\left(\frac{4QTP_bZ}{\pi T_b D^2}\right)^2\int_0^t dt - \frac{f}{2g_c D}\left(\frac{4QTP_bZ}{\pi T_b D^2}\right)^2\int_0^L dx\int_0^t dt \tag{23}$$

By integrating Equation (23), the following equation could be obtained:

$$\left(\frac{RZT}{Mw_a\gamma_g}\right)\left(\frac{P_1^2 - P_2^2}{2}\right)\Delta t = \frac{1}{2g_c}\left(\frac{4QTP_bZ}{\pi T_b D^2}\right)^2 L + \frac{1}{2g_c}\left(\frac{4QTP_bZ}{\pi T_b D^2}\right)^2\Delta t + \frac{f}{2g_c}\left(\frac{4QTP_bZ}{\pi T_b D^2}\right)^2\frac{L\Delta t}{D} \tag{24}$$

Substituting $g_c = 1$ kg. m/N. s^2, $R = 8.314$ kJ/kmol. K , Mw_a in Equation $= 29$ kg/kmol (24) and simplifying the terms, the unsteady natural gas flow rate in a pipeline is achieved as:

$$Q = \sqrt{\frac{8.314}{29\times10^3\times\left(\frac{4\times10^3}{\pi}\right)^2}}\left(\frac{T_b}{P_b}\right)\sqrt{\frac{(P_1^2 - P_2^2)}{ZT\gamma_g}D^5\left[\frac{\Delta t}{fL\Delta t + \frac{D\Delta t}{10^6} + \frac{DL}{10^3}}\right]} \tag{25}$$

Where Q is the volumetric flow rate (m^3/s), D represents the pipeline diameter (mm), L shows the pipeline length (km), T denotes the average natural gas temperature (K), Δt stands for the time change (s) and P is the natural gas pressure (kPa). Finally, Equation (25) could be made simpler and converted to Equation (26) as:

$$Q = 1.329\times10^{-8}\left(\frac{T_b}{P_b}\right)\sqrt{\frac{(P_1^2 - P_2^2)}{ZT\gamma_g}D^5\left[\frac{\Delta t}{fL\Delta t + \frac{D\Delta t}{10^6} + \frac{DL}{10^3}}\right]} \tag{26}$$

Equation (26) could also be rewritten as follows:

$$P_1^2 - P_2^2 = K(t)\ Q^2 \tag{27}$$

Where $K(t)$ is defined as the following equation:

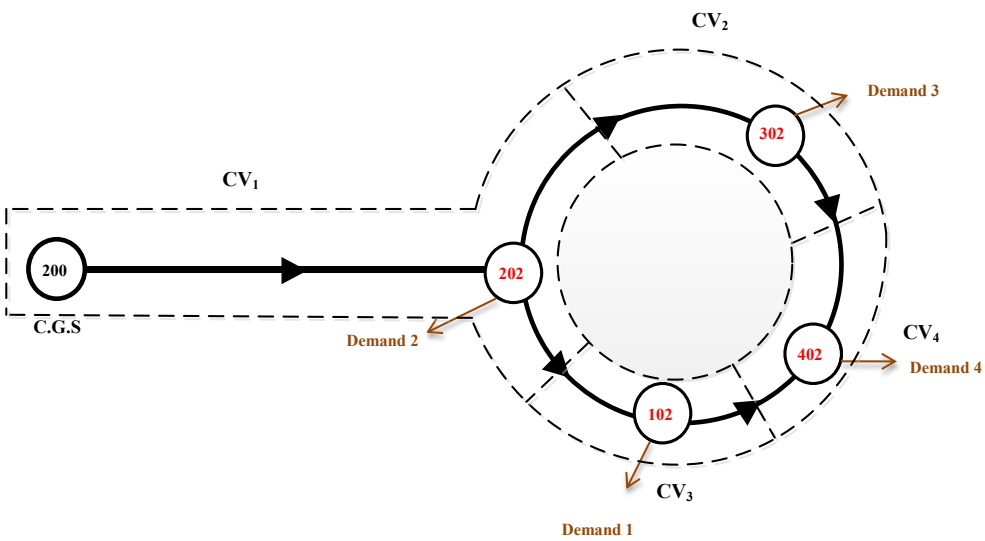

Fig. 8. Control volumes for the pipeline network under unsteady conditions.

$$K(t) = \left(\frac{P_b}{1.329 \times 10^{-8} T_b}\right)^2 \left[\left(\frac{ZT\gamma_g}{D^5}\right) \times \left(\frac{fL\Delta t + \frac{D\Delta t}{10^6} + \frac{DL}{10^3}}{\Delta t}\right)\right] \tag{28}$$

To analyze the unsteady natural gas pipeline network, a new approach has been employed in the present study. In this approach, natural gas storage in the pipeline junction is possible. Fig. 8 illustrates the control volumes for each node with capability of storing natural gas. Considering this assumption, natural gas can be consumed from the stored gas in pipelines. This is the so-called natural gas accumulation mode. The conservation of mass equation in the unsteady-state condition for each node is presented as follows:

$$\frac{dm_j}{dt} = \sum_{i=1}^{Np} K_{ij}(\dot{m}_{ij} - \dot{m}_j) \tag{29}$$

In which m_j shows the amount of storage natural gas in node j, $\dot{m}_{ij}$ refers to the mass flow into or out of node j by the pipeline connected to the node, $\dot{m}_j$ shows the mass flow consumed by node j, Np is the number of pipelines connected to node j and K_{ij} equals 1 if the flow enters and equals −1 if the flow leaves the node.

The left hand side of Equation (29) could be rewritten as follows:

$$\frac{dm}{dt} = \frac{d(\rho V)}{dt} = \left(\frac{V}{ZRT}\right)\frac{dP}{dt} \tag{30}$$

Where V is volume. Combining Equations (29) and (30) and converting mass flow rate into volumetric flow rate, then, Equation (31) could be driven as:

$$\left(\frac{V}{ZRT}\right)\frac{dP_j}{dt} = \sum_{i=1}^{Np} K_{ij} \times \rho_b \times (Q_{ij} - NGD_j) \tag{31}$$

Where, ρ_b is the density in the base condition, Q is the volumetric flow in the pipeline connected to node and NGD is the natural gas demand in the specific node.

By discretizing Equation (31), the following equation could be obtained:

$$\left(\frac{V}{ZRT}\right)\frac{P_j^{k+1} - P_j^k}{\Delta t} = \sum_{i=1}^{Np} K_{ij} \times \rho^* \times \left(1.329 \times 10^{-8}\left(\frac{T_b}{P_b}\right) \times \sqrt{\frac{(Pi^{2(k+1)} - Pj^{2(k+1)})}{ZT\gamma_g} D^5 \left[\frac{\Delta t}{fL\Delta t + \frac{D\Delta t}{10^6} + \frac{DL}{10^3}}\right]} - Q_j\right) \tag{32}$$

According to Equation (32), the pressure in the next time step, k + 1, should be calculated from the previous time k. By applying Equation (32) for all the network nodes, a system of nonlinear equations with $\underline{M}$ equations and M unknowns will be obtained. $\underline{M}$ is the number of pipeline network nodes. Here, the system of nonlinear equations have been solved by applying MATLAB® software as well as Optimization Toolbox for each time interval. Afterwards, the pressure at nodes has been calculated.

The discussed proposed algorithm model for analyzing the natural gas distribution pipeline network under the unsteady conditions could be summarized as follows:

1. Each node and a section of pipeline connected to the node were considered as the control volume.
2. The conservation of mass equation in the unsteady conditions (Equation (29)) was applied for each control volume of each node.
3. Using Equation (26), the flow rate in a pipeline was calculated and, as a result, a differential equation was derived for each node.
4. The differential equation for each node was discretized according to boundary conditions (natural gas demand). The pressure of each node at the next time step was calculated according to the specified conditions.

6. Results and discussion

In this section, the natural gas distribution pipeline under investigation (See Fig. 1) is first analyzed under the steady state condition. The mass flow rate in pipelines and pressure at nodes are calculated in this condition. The natural gas demands for any nodes are calculated by knowing the number of users connected to the node and ambient temperature. Then, considering steady state results as the initial condition, the response of the distribution network due to ATV is calculated under the unsteady condition.

6.1. Steady state results

Table 3 shows the natural gas flow rate in each pipeline and Table 4 indicates the pressure at each node of the pipeline network in the steady state condition. In the steady state condition, the ambient temperature is kept constant at 15 °C.

6.2. Effect of ambient temperature variation

Table 5 presents the hourly ambient temperature variation for the

Table 3
The natural gas volumetric flow rate of the pipeline network at the steady state condition.

Flow rate ID	from node	to node	flow rate (m^3/h)
Q_0	200	202	31300
Q_1	202	102	14452.8
Q_2	202	302	11847.2
Q_3	302	402	6847.2
Q_4	102	402	9452.8

Table 4
The natural gas pressure for each node at the steady state condition.

Node	pressure (kPa)
200	1723.8
102	1705.54
202	1710.28
302	1703.27
402	1697.2

Table 5
Hourly ambient temperature for the four coldest days of 2013.

Time (hour)	case day 1	case day 2	case day 3	case day 4
	ambient temperature (°C)			
1	0.775862	1.206897	**−1.50862**	0.12931
2	0.258621	0.646552	−1.46552	−0.08621
3	−0.21552	0.086207	−1.37931	−0.34483
4	−0.51724	−0.25862	−1.37931	−0.47414
5	−0.81897	−0.56034	−1.37931	−0.60345
6	−1.03448	−0.81897	−1.33621	**−0.68966**
7	−1.12069	−0.81897	−1.25	−0.60345
8	−0.77586	−0.25862	−0.30172	0.12931
9	−0.38793	0.301724	0.646552	0.905172
10	0	0.818966	1.508621	1.637931
11	0.301724	1.25	2.198276	2.241379
12	0.474138	1.551724	2.672414	2.715517
13	0.603448	1.724138	3.017241	3.060345
14	0.560345	1.767241	3.146552	3.189655
15	0.431034	1.681034	3.103448	3.146552
16	0.172414	1.37931	2.758621	2.801724
17	−0.25862	0.905172	2.241379	2.241379
18	−0.43103	0.431034	1.637931	2.025862
19	−0.64655	0.086207	1.551724	1.810345
20	−0.81897	−0.25862	1.508621	1.594828
21	−0.99138	−0.56034	1.422414	1.336207
22	−1.16379	−0.90517	1.336207	1.12069
23	−1.37931	−1.2069	1.293103	0.905172
24	**−1.55172**	**−1.55172**	1.206897	0.689655

four coldest days of 2013. The lowest ambient temperature for each day is shown in bold font. According to Table 5, ambient temperature had the lowest value at about 12 p.m., 1 a.m. and 6 a.m. for days 1 and 2, day 3 and day 4 respectively. The highest ambient temperature occurred at 3 p.m. As it could be realized, the temperature follows a sinusoids trend except for day 3.

Fig. 9 demonstrates the variation of natural gas demand versus time for the selected four days in 2013. The natural gas demand has been presented for all users. In this study, it is assumed that natural gas demand is equally divided on the nodes. Considering the information presented in Table 5, it could be realized that natural gas demand (Fig. 9) follows the ATV. As ambient temperature increases, the demand decreases and vice versa.

The pressure in the natural gas distribution pipeline network nodes is a key parameter and should be monitored at any time. The response of the natural gas distribution pipeline network to ATV is the same as pressure variation at network nodes. Therefore, in this section, the

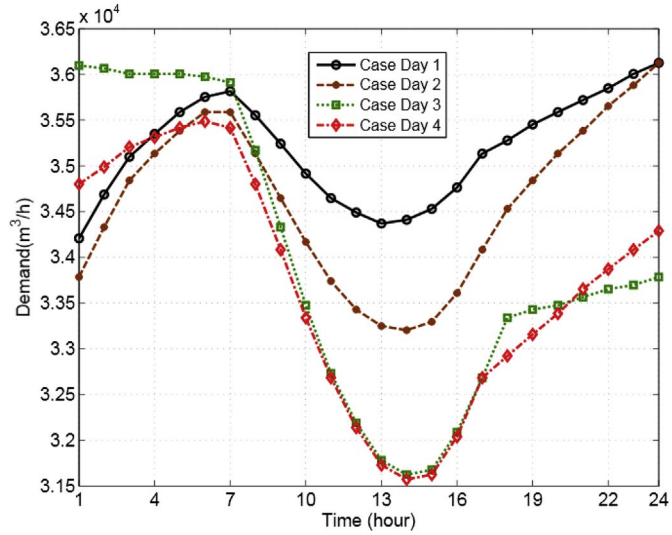

Fig. 9. Variation of natural gas demand versus time for the selected four days in 2013.

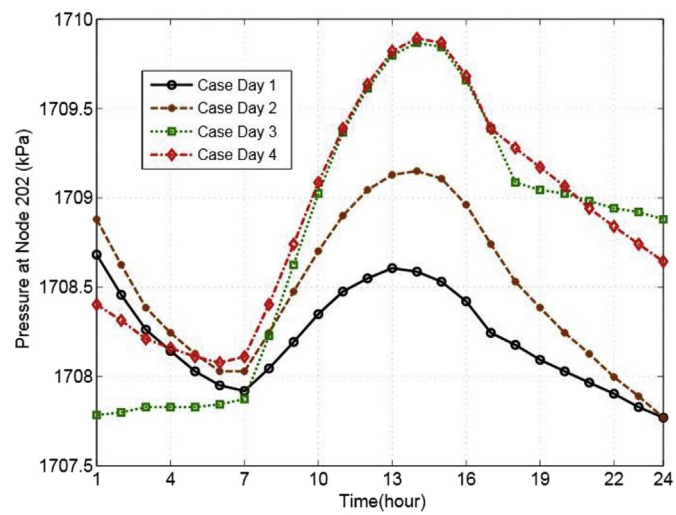

Fig. 10. Variation of pressure at node 202 versus time for the selected four days in 2013.

pressure at natural gas pipeline network nodes have been calculated and presented. Fig. 10 shows the hourly pressure at node 202 as the source node in the network. The pressure has been depicted for the four coldest days of 2013. According to Fig. 10, the ATV affects the pressure at node 202. By increasing the demand at node 202, the pressure is decreased and vice versa. The decrease in pressure at node 202 is small (about 1%) as the pipeline diameter between source node 200 and node 202 is high which allows more natural gas flows through it.

Fig. 11 presents the hourly pressure at nodes in the natural gas pipeline network. The day 3 has been selected for natural gas node demands. According to Fig. 11, the ATV affects the node pressure. The highest pressure drop at nodes occurs in day 3 in which the natural gas demand is maximum. The pressure drop at node 302 relative to the steady state is minimum in the distribution pipeline network due to the higher amount of natural gas stored in natural gas pipeline ID 0 and 2. The decrease in pressure at node 402 is the highest (about 2%) since the natural gas demand at node 402 is maximum compared with the other nodes.

Fig. 12 shows the maximum amount of inlet flow rate (gas pipe ID 0) for the selected four days in 2013. The highest flow rate occurs at a time when demand is minimum (see Fig. 9). According to Fig. 12 as demand increases, the flow rate increases as well. Based on Figs. 9 and 12, by increasing natural gas demand at any node, the pressure at that

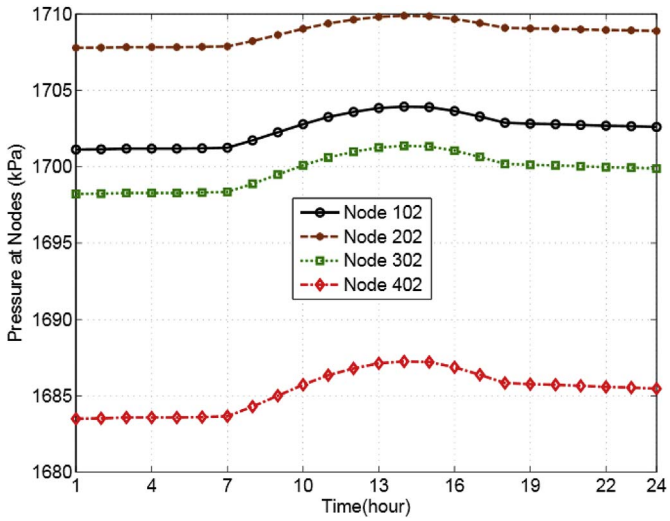

Fig. 11. Variation of pressure at nodes versus time for Case Day 3 in 2013.

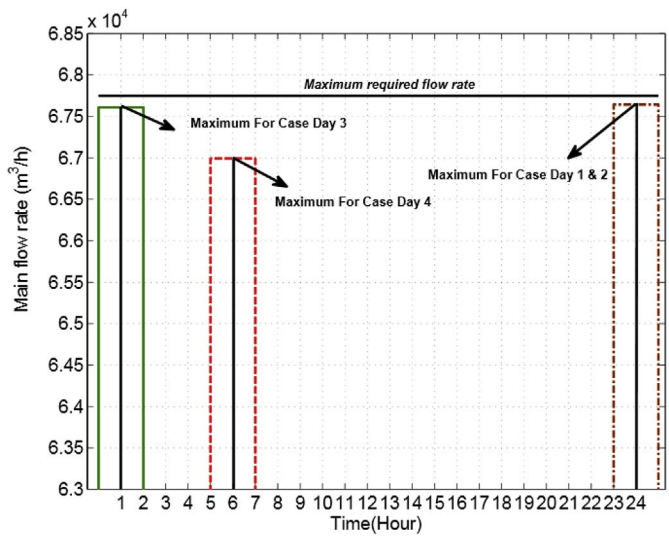

Fig. 12. Maximum main flow rate for the selected four days in 2013.

node decreases but the flow rate in the pipeline increases.

Fig. 13 illustrates the variation of natural gas flow velocity in the main pipeline (gas pipe ID 0) versus time for the selected four days of 2013. The velocity within the pipeline should be kept below a certain value (18 m/s) to prevent corrosion (Standards and Research Department, 2003). According to Fig. 13, the natural gas velocity is approximately 8 m/s, much lower than the critical value.

6.3. Effect of natural gas composition

Natural gas is a mixture of several components with various properties. In this section, the effect of natural gas composition has been studied on the pressure at nodes and natural gas flow rate in pipelines. Table 6 lists the mole fraction of natural gas for Iran's field used in the present study. These natural gases were studied because of the greatest difference in their compositions.

In this section, the effect of natural gas composition has been studied in the pipeline network. Fig. 14 demonstrates the variation of pressure at node 202 versus hour for various natural gases in the maximum demand. According to Fig. 14, by increasing the molecular weights of natural gas, the pressure at nodes decreases. This is due to the increase in specific gravity of natural gas, which caused further pressure drop in pipelines and consequently, a lower pressure at nodes.

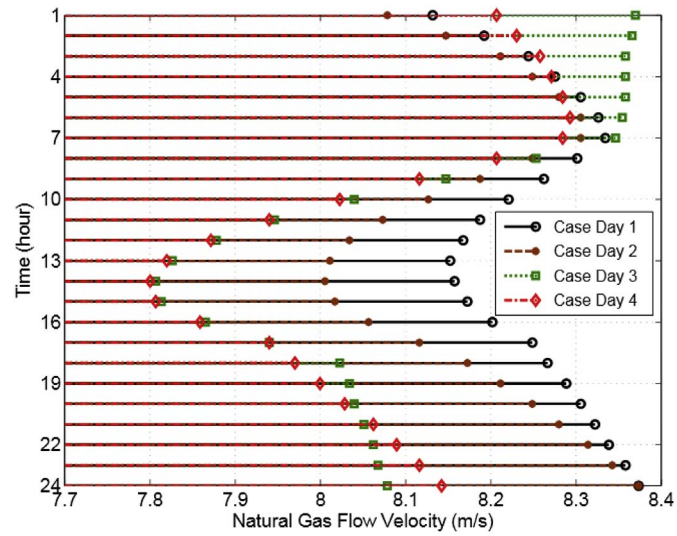

Fig. 13. Variation of natural gas velocity versus time for the selected four days in 2013.

Table 6
Mole fraction of natural gas extracted from various regions of Iran (National Iran Gas Company official website).

Component	mole fraction (%)		
	Khangiran	Kangan	Pars
CH_4	98.6	90.04	87
C_2H_6	0.59	3.69	5.4
C_3H_8	0.09	0.93	1.7
i-C_4H_{10}	0.02	0.2	0.3
n-C_4H_{10}	0.04	0.29	0.45
i-C_5H_{12}	0.02	0.14	0.13
n-C_5H_{12}	0.02	0.08	0.11
n-C_6H_{14}	0.07	0.14	0.07
C_7^+	0	0.01	0.03
N_2	0.56	4.48	3.1
CO_2	0	0	1.85
molecular weights (kg/kmol)	16.31	17.79	18.68

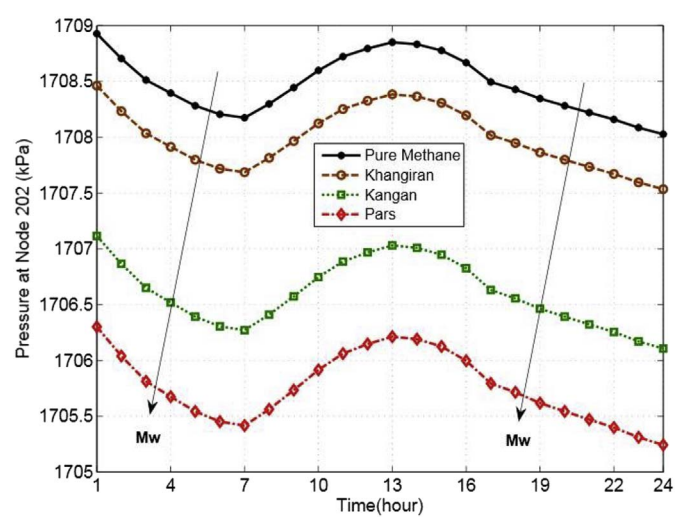

Fig. 14. Variation of pressure at Node 202 versus time for various natural gases in the maximum demand for 2013.

Fig. 15 shows the variation of the main flow rate versus time for various natural gases in the maximum demand for 2013. According to Fig. 15, by increasing the molecular weights, the main flow rate increases due to increase in natural gas pressure drop in pipes.

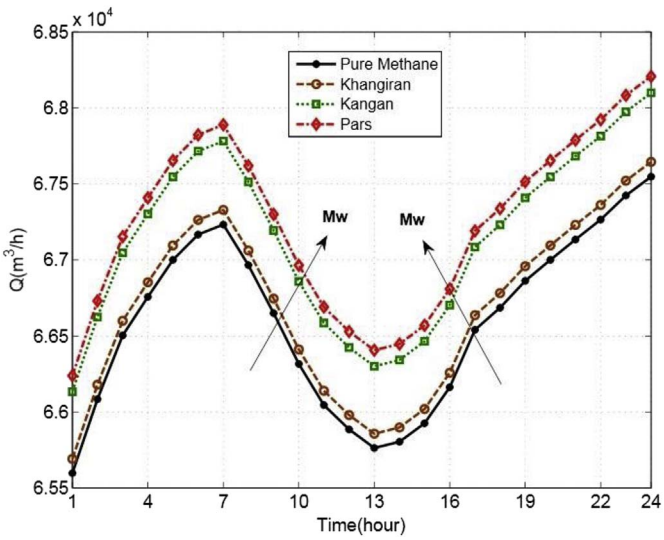

Fig. 15. Variation of the main flow rate versus time for various natural gases in the maximum demand for 2013.

7. Conclusions

The main purpose of this study was to investigate the effects of ATV on the important parameters of natural gas distribution pipeline network including node pressures and in-pipe velocities. To achieve this goal, firstly, a model has been developed to forecast natural gas demand at any ambient temperature by applying the MLP neural network. Then, the distribution network has been modeled under the steady condition and the calculated results were assumed as the initial condition of unsteady modeling. Finally, the distribution network has been simulated under the unsteady conditions. The model has been applied for a selected city (Semnan) to determine the response of the network in the four cold days. The results revealed that the method proposed for forecasting natural gas demand has an error of about 1% compared with the measured values. In addition, the simulation results of the networks indicate that, in the coldest day of the year, the pressure at nodes is significantly dropped due to an increase in natural gas demand. The effect of natural gas composition on node pressure was also studied and the results showed that natural gases with higher molecular weights have a lower pressure in all network nodes.

Acknowledgment

The authors would like to thank the officials in Semnan Gas Company for providing financial support for this research.

Appendix A. Real Gas Effect

In this work, natural gas has been assumed as a real gas and the AGA8 equation of state (EOS) has been employed to compute its properties The AGA8 EOS was originally developed for predicting the compression factor and density of natural gas. This EOS is basically used in custody transfer. The AGA8 report assumes natural gas as mixture of 21 components. The AGA8 EOS could be employed for the temperature range of 143–675 K and pressure range of 0–280 MPa (AGA8–DC92 EoS, 1992). The AGA8 EOS was incorporated by Farzaneh-Gord and Rahbari (Farzaneh-Gord and Rahbari, 2012, 2011) to develop approaches to compute the thermodynamic properties of natural gas. Based on the AGA8 EOS and thermodynamic relationship, enthalpy, entropy, and other thermodynamic properties were calculated and reported.

The basic equation of AGA8 EOS for calculating the compression factor is defined as follows (AGA8–DC92 EoS, 1992):

$$Z = 1 + B\rho_m - \rho_r \sum_{n=13}^{18} C_n^* + \sum_{n=13}^{58} C_n^* D_n^* \tag{A1}$$

In which ρ_r is the reduced density defined as follows:

$$\rho_r = K^3 \rho_m \tag{A2}$$

In Equation (A2), ρ_m is the molar density and K is the mixture size parameter. Parameter K is defined by the following equation (AGA8–DC92 EoS, 1992):

$$K^5 = \left(\sum_{i=1}^{N} x_i K_i^{\frac{5}{2}} \right)^2 + 2 \sum_{i=1}^{N-1} \sum_{j=i+1}^{N} x_i x_j (K_{ij}^5 - 1)(K_i K_j)^{\frac{5}{2}} \tag{A3}$$

where x_i is the mole fraction of component i in the mixture, x_j is the mole fraction of component j in the mixture, K_i is the size parameter of component i, K_j is the size parameter of component j, K_{ij} is the binary interaction parameter for size, and N is the number of compositions in the natural gas mixture.

Parameter B in Equation (A1) is defined by the following equation (AGA8–DC92 EoS, 1992):

$$B = \sum_{n=1}^{18} a_n T^{-u_n} \sum_{i=1}^{N} \sum_{j=1}^{N} x_i x_j B_{nij}^* E_{ij}^{u_n} (K_i K_j)^{\frac{3}{2}} \tag{A4}$$

Parameter B_{nij}^* is defined by Equation (A5) and parameter E_{ij} is defined by Equation (A6) (AGA8–DC92 EoS, 1992):

$$B_{nij}^* = (G_{ij} + 1 - g_n)^{g_n} (Q_i Q_j + 1 - q_n)^{q_n} (F_i^{1/2} F_j^{1/2} + 1 - f_n)^{f_n} (S_i S_j + 1 - s_n)^{s_n} (W_i W_j + 1 - w_n)^{w_n} \tag{A5}$$

$$E_{ij} = E_{ij}^* (E_i E_j)^{1/2} \tag{A6}$$

G_{ij} in Equation (A5) is defined as follows (AGA8–DC92 EoS, 1992):

$$G_{ij} = \frac{G_{ij}^* (G_i + G_j)}{2} \tag{A7}$$

The parameters in Equations (A4) to (A7) include T denoting temperature, N showing the number of components in gas mixture, a_n, f_n, g_n, q_n, s_n,

u_n, w_n representing the equation of state parameters, E_i, F_i, G_i, K_i, Q_i, S_i, W_i referring to the corresponding characterization parameters, and E_{ij}^*, G_{ij}^*indicating the corresponding binary interaction parameters.

The coefficient C_n^*; $n = 1, \ldots, 58$ in Equation (A1) is defined as (AGA8–DC92 EoS, 1992):

$$C_n^* = a_n(G + 1 - g_n)^{g_n}(Q^2 + 1 - q_n)^{q_n}(F + 1 - f_n)^{f_n} U_n^{u_n} T^{-u_n} \tag{A8}$$

Where G, F, Q, U are mixture parameters defined by Equations (A9) to (A12) (AGA8–DC92 EoS, 1992):

$$U^5 = \left(\sum_{i=1}^{N} x_i E_i^{\frac{5}{2}}\right)^2 + 2\sum_{i=1}^{N-1}\sum_{j=i+1}^{N} x_i x_j (U_{ij}^5 - 1)(E_i E_j)^{\frac{5}{2}} \tag{A9}$$

$$G = \sum_{i=1}^{N} x_i G_i + 2\sum_{i=1}^{N-1}\sum_{j=i+1}^{N} x_i x_j (G_{ij}^* - 1)(G_i + G_j) \tag{A10}$$

$$Q = \sum_{i=1}^{N} x_i Q_i \tag{A11}$$

$$F = \sum_{i=1}^{N} x_i^2 F_i \tag{A12}$$

In equation (A9), U_{ij} denotes the binary interaction parameter for mixture energy. Moreover, in Equation (A1), D_n^* is defined by the following equation:

$$D_n^* = \left(b_n - c_n k_n \rho_r^{k_n}\right)\rho_r^{b_n} \exp\left(-c_n \rho_r^{k_n}\right) \tag{A13}$$

Coefficients of all parameters in the above equations are presented in reference (AGA8–DC92 EoS, 1992). By knowing the mole fraction of natural gas composition, temperature, and pressure, the compression factor and density of natural gas could be calculated by applying AGA8 EOS.

References

Adeosun, T.A., Olatunde, O.A., Aderohunmu, J.O., Ogunjare, T.O., 2009. Development of unsteady-state Weymouth equations for gas volumetric flow rate in horizontal and inclined pipes. J. Nat. Gas Sci. Eng. 1, 113–117.

Adewumi, M.A., Zhou, J., 1995. Simulation of transient flow in natural gas pipelines. In: PSIG Annual Meeting. Pipeline Simulation Interest Group.

AGA8–DC92 EoS, 1992. Compressibility and Super Compressibility for Natural Gas and Other Hydrocarbon Gases. Transmission Measurement Committee Report No. 8, AGA Catalog No. XQ 1285, Arlington, VA.

Alamian, R., Behbahani-Nejad, M., Ghanbarzadeh, A., 2012. A state space model for transient flow simulation in natural gas pipelines. J. Nat. Gas Sci. Eng. 9, 51–59.

Aydinalp-Koksal, M., Ugursal, V.I., 2008. Comparison of neural network, conditional demand analysis, and engineering approaches for modeling end-use energy consumption in the residential sector. Appl. Energy 85, 271–296.

Behbahani-Nejad, M., Bagheri, A., 2010. The accuracy and efficiency of a MATLAB-Simulink library for transient flow simulation of gas pipelines and networks. J. Petrol. Sci. Eng. 70, 256–265.

Behbahani-Nejad, M., Shekari, Y., 2010. The accuracy and efficiency of a reduced-order model for transient flow analysis in gas pipelines. J. Petrol. Sci. Eng. 73, 13–19.

Behrooz, H.A., Boozarjomehry, R.B., 2015. Modeling and state estimation for gas transmission networks. J. Nat. Gas Sci. Eng. 22, 551–570.

Chaczykowski, M., 2010. Transient flow in natural gas pipeline–The effect of pipeline thermal model. Appl. Math. Model. 34, 1051–1067.

Chaczykowski, M., 2009. Sensitivity of pipeline gas flow model to the selection of the equation of state. Chem. Eng. Res. Des. 87, 1596–1603.

DEMİREL, Ö.F., Zaim, S., Çalişkan, A., Özuyar, P., 2012. Forecasting natural gas consumption in Istanbul using neural networks and multivariate time series methods. Turk. J. Electr. Eng. Comput. Sci. 20, 695–711.

Dukhovnaya, Y., Adewumi, M.A., 2000. Simulation of non-isothermal transients in gas/condensate pipelines using TVD scheme. Powder Technol. 112, 163–171.

Ebrahimzadeh, E., Shahrak, M.N., Bazooyar, B., 2012. Simulation of transient gas flow using the orthogonal collocation method. Chem. Eng. Res. Des. 90, 1701–1710.

Farzaneh-Gord, M., Rahbari, H.R., 2016. Unsteady natural gas flow within pipeline network, an analytical approach. J. Nat. Gas Sci. Eng. 28.

Farzaneh-Gord, M., Rahbari, H.R., 2012. Numerical procedures for natural gas accurate thermodynamic properties calculation. J. Eng. Thermophys. 21.

Farzaneh-Gord, M., Rahbari, H.R., 2011. Developing novel correlations for calculating natural gas thermodynamic properties. Chem. Process Eng. - Inz. Chem. i Proces 32, 435–452.

Gato, L.M.C., Henriques, J.C.C., 2005. Dynamic behaviour of high-pressure natural-gas flow in pipelines. Int. J. Heat Fluid Flow 26, 817–825.

Gorucu, F.B., 2004. Artificial neural network modeling for forecasting gas consumption. Energy Sources 26, 299–307.

Greyvenstein, G.P., 2002. An implicit method for the analysis of transient flows in pipe networks. Int. J. Numer. Meth. Eng. 53, 1127–1143.

Haaland, S.E., 1983. Simple and explicit formulas for the friction factor in turbulent pipe flow. J. Fluid Eng. 105, 89–90.

Helgaker, J.F., Oosterkamp, A., Langelandsvik, L.I., Ytrehus, T., 2014. Validation of 1D flow model for high pressure offshore natural gas pipelines. J. Nat. Gas Sci. Eng. 16, 44–56.

Herrán-González, A., De La Cruz, J.M., De Andrés-Toro, B., Risco-Martín, J.L., 2009. Modeling and simulation of a gas distribution pipeline network. Appl. Math. Model. 33, 1584–1600.

I.R.OF IRAN Meteorological Organization website, http://www.irimo.ir/eng/index.php.

Ibraheem, S.O., Adewumi, M.A., 1996. Higher-resolution numerical solution for 2-D transient natural gas pipeline flows. In: SPE Gas Technology Symposium. Society of Petroleum Engineers.

Kavaklioglu, K., Ceylan, H., Ozturk, H.K., Canyurt, O.E., 2009. Modeling and prediction of Turkey's electricity consumption using artificial neural networks. Energy Convers. Manag. 50, 2719–2727.

Ke, S.L., Ti, H.C., 2000. Transient analysis of isothermal gas flow in pipeline network. Chem. Eng. J. 76, 169–177.

Khotanzad, A., Elragal, H., Lu, T.-L., 2000. Combination of artificial neural-network forecasters for prediction of natural gas consumption. IEEE Trans. Neural Network. 11, 464–473.

Kiuchi, T., 1994. An implicit method for transient gas flows in pipe networks. Int. J. Heat Fluid Flow 15, 378–383.

Kizilaslan, R., Karlik, B., 2009. Combination of neural networks forecasters for monthly natural gas consumption prediction. Neural Netw. World 19, 191.

Kolomogorov, A.N., Fomin, S.V., 1957. Element of the theory of functions and functions analysis. Metric and Normed Spaces 1.

Kovačič, M., Šarler, B., 2014. Genetic programming prediction of the natural gas consumption in a steel plant. Energy 66, 273–284.

Luongo, C.A., others, 1986. An efficient program for transient flow simulation in natural gas pipelines. In: PSIG Annual Meeting.

National Iran Gas Company official website, http://nigc.com/pages/Products.html.

Olatunde, A.O., Adeosun, T.A., Usman, M.A., Odunlami, O.M., Olowofoyeku, M.A., Ekakitie, T.E., Mohammed, A.M., 2012. Direct calculation of unsteady-state Weymouth equations for gas volumetric flow rate with different friction factors in horizontal and inclined pipes. Engineering 4, 202.

Osiadacz, A., 1987. Simulation and Analysis of Gas Networks.

Osiadacz, A., 1983. Optimal numerical method for simulating dynamic flow of gas in pipelines. Int. J. Numer. Meth. Fluid. 3, 125–135.

Osiadacz, A.J., Chaczykowski, M., 2001. Comparison of isothermal and non-isothermal pipeline gas flow models. Chem. Eng. J. 81, 41–51.

Potočnik, P., Soldo, B., Šimunović, G., Šarić, T., Jeromen, A., Govekar, E., 2014. Comparison of static and adaptive models for short-term residential natural gas forecasting in Croatia. Appl. Energy 129, 94–103.

Reddy, H.P., Narasimhan, S., Bhallamudi, S.M., 2006. Simulation and state estimation of transient flow in gas pipeline networks using a transfer function model. Ind. Eng. Chem. Res. 45, 3853–3863.

Shashi Menon, E., 2005. Gas Pipeline Hydraulics.

Szoplik, J., 2015. Forecasting of natural gas consumption with artificial neural networks. Energy 85, 208–220.

Tao, W.Q., Ti, H.C., 1998. Transient analysis of gas pipeline network. Chem. Eng. J. 69, 47–52.

Tentis, E., Margaris, D., Papanikas, D., 2003. Transient gas flow simulation using an adaptive method of lines. Comptes Rendus Mec 331, 481–487.

Wang, P., Yu, B., Deng, Y., Zhao, Y., 2015. Comparison study on the accuracy and efficiency of the four forms of hydraulic equation of a natural gas pipeline based on linearized solution. J. Nat. Gas Sci. Eng. 22, 235–244.
Wylie, E.B., Stoner, M.A., Streeter, V.L., 1971. Network: system transient calculations by implicit method. Soc. Petrol. Eng. J. 11, 356–362.
Wylie, E.B., Streeter, V.L., 1993. Fluid Transients in Systems (PrenticeHall Upper Saddle River NJ). .
Yow, W., 1971. Analysis and Control of Transient Flow in Natural Gas Piping Systems.
Yu, F., Xu, X., 2014. A short-term load forecasting model of natural gas based on optimized genetic algorithm and improved BP neural network. Appl. Energy 134, 102–113.

Nomenclature

b: bias vector
D: pipe inside diameter (mm)
f: friction factor
Δt: change in time (second)
L: pipe length (km)
ṁ: mass flow rate (kg/s)
g_c*:* gravitational conversion factor
M: number of pipeline network nodes
Mw: molecular weights (kg/kmol)
N: number of data
Np: number of pipelines
n: Haaland equation parameter n = 3
P: pressure (kPa)
Q: volumetric Flow Rate (m^3/s)
R: gas constant (kJ/kmol.K)

R-squared Regression Values

T: Temperature (K or ^oC)
u: velocity (m/s)
V: volume (m^3)
W: weight matrix
x: spatial position
Z: compression factor

Subscript

a: air
act: actual
b: base condition
g: gas
fcst: forecast
1: up stream
2: down stream

Greek Letters

ρ: Density (kg/m^3)
γ: Gas specific gravity
ε: Pipeline roughness

Abbreviations

ANN: Artificial Neural Network
ATV: Ambient Temperature Variation
CGS: City Gate Station
EOS: Equation of State
MLP: Multilayer Perceptron
MSE: Mean Square Error
NGD: Natural Gas Demand
TBS: Town Border Station

AGA8 EOS Parameters

B: Second Virial coefficient
C_n^**:* temperature and composition dependent coefficient
K_j*:* size parameter of component *j*
K_{ij}*:* binary interaction parameter
N: number of component in gas mixture
x: mole fraction of component
E_{ij}^**:* binary energy interaction parameter for second virial coefficient
E_i*:* characterization energy parameter for *i*-th component (K)
E_{ij}*:* binary energy parameter for second virial coefficient (K)
F: mixture high-temperature parameter
F_i*:* high-temperature parameter for *i*-th component
G: mixture orientation parameter
G_{ij}^**:* binary interaction parameter for orientation
Q: quadrupole parameter
U_{ij}*:* binary interaction parameter for mixture energy
W_i*:* association parameter for *i*-th component -
ρ_m*:* molar density (kmol/m^3)
ρ_r*:* reduce density (kmol/m^3)